SCIENCE CHINA
Information Sciences

January 2019, Vol. 62 010204:1–010204:10
https://doi.org/10.1007/s11432-018-9579-3

• RESEARCH PAPER •
Special Focus on Guidance, Navigation and Control

Cooperative geometric localization for a ground target based on the relative distances by multiple UAVs

Yaohong QU*, Feng ZHANG, Xiwei WU & Bing XIAO

School of Automation, Northwestern Polytechnical University, Xi'an 710072, *China*

Received 27 June 2018/Accepted 19 July 2018/Published online 20 December 2018

Abstract Based on the locations of several unmanned aerial vehicles (UAVs) and their relative distances from a target, a ground target cooperative geometric localization method that is more effective than a traditional approach is proposed in this paper. First, an algorithm for determining the location of the target is described. The effectiveness and suitability of the proposed algorithm are then shown. Next, to investigate the location accuracy of the proposed method, the influence of three critical factors, namely, the flight altitude, UAV position errors, and measurement errors, is analyzed. Furthermore, for the required location accuracy, the feasible regions of these factors are determined based on their influence, and the location accuracy will satisfy the requirements if all factors are within the feasible regions. Finally, simulation results from the MATLAB/Simulink toolbox are presented to show the effectiveness of the proposed method and the availability of the feasible regions.

Keywords unmanned aerial vehicle, UAV, relative distance, cooperative localization, location effectiveness analysis, feasible regions

Citation Qu Y H, Zhang F, Wu X W, et al. Cooperative geometric localization for a ground target based on the relative distances by multiple UAVs. Sci China Inf Sci, 2019, 62(1): 010204, https://doi.org/10.1007/s11432-018-9579-3

1 Introduction

Locating a ground target using a UAV has attracted considerable attention in many research fields owing to its prominent advantages [1–3]. A single UAV was used to estimate the location of a target in the past [4,5], but it cannot satisfy the higher precision requirements. The determination of a target location through the cooperative use of multiple UAVs has recently appeared, and has rapidly become a high-precision location method [6,7].

Cooperative localization is increasingly being used by the military and in scientific research fields [8]. An increasing number of scholars have conducted studies in this area and have achieved fruitful results. The constrained total least-squares location algorithm using time-difference-of-arrival (TDOA) measurements, as proposed by Yang et al. [9], achieves a high level of accuracy; however, it does so by ignoring the location errors of the observers. Similarly, a method proposed by Niculescu [10] has the same disadvantage. A TOA localization algorithm proposed by Zhu et al. [11] achieves a high location accuracy when the sensor location information is precisely known; however, once random location errors occur, its position performance drops sharply. Moreover, an algorithm proposed by Grewal et al. [12], which estimates the target location by utilizing the relative distances and position of the observers, also neglects their location

* Corresponding author (email: qyh0809@nwpu.edu.cn)

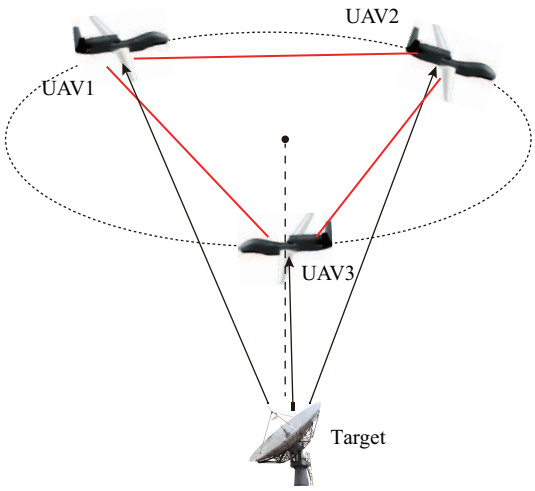

Figure 1 (Color online) Example of cooperative localization using three UAVs.

errors. The above methods are unable to adapt to situations in which the location errors of the observers are too large to ignore; in other words, it is necessary to investigate an algorithm that is more effective and suitable for cooperative localization.

The proposed method ensures high positioning accuracy and resolves the influence of position errors of the UAVs synchronously, which is inspired by the study in [13]. The main contributions of this paper are as follows:

(a) A cooperative localization method is proposed, the effectiveness and suitability of which are proven through simulation results.

(b) Feasible regions of the flight altitude, UAV position errors, and measurement errors are determined for the specific requirements of the location accuracy, providing a good location window for reference.

2 Location calculation

2.1 Problem formulation

Assume that multiple UAVs, which are equipped with a GPS receiver and a ranging sensor, circle around the same target. The position coordinates of each UAV can then be obtained using the GPS receiver, and the relative distances from each UAV to the target can be measured using the ranging sensor. An example of cooperative localization using three UAVs is shown in Figure 1.

2.2 Location and calculation

The main idea of location algorithm is as follows:

Step 1. The initial location $\boldsymbol{x}_0$ of the target is calculated using the initial location algorithm [12].

Step 2. Localization equations based on measurement errors are expanded in a Taylor series regarding a certain nominal solution $\boldsymbol{x}_0$, and the expression of the location solution can be deduced through the proposed algorithm.

Step 3. The λ parameter in the expression of the location can be solved using an approximate solution for the singular value decomposition, and the target location can be obtained by substituting λ into the expression.

2.2.1 *Initial location* $\boldsymbol{x_0}$

In an earth-centered inertial coordinate system, the relative distances ρ_i from the target to each UAV, which has known coordinates $\boldsymbol{x}_i = [x_i, y_i, z_i]^{\mathrm{T}}$ (where $i = 1, 2, 3$), and unknown target coordinates

$\boldsymbol{x}_t = [x_t, y_t, z_t]^{\mathrm{T}}$, are given by

$$\rho_i = \|\boldsymbol{x}_i - \boldsymbol{x}_t\| = \sqrt{(x_i - x_t)^2 + (y_i - y_t)^2 + (z_i - z_t)^2}, \tag{1}$$

where i denotes the index of the UAVs, as shown in Figure 1, and at least three UAVs are required. Let

$$\begin{cases} r^2 = ({x_t}^2 + {y_t}^2 + {z_t}^2), \\ {r_i}^2 = ({x_i}^2 + {y_i}^2 + {z_i}^2), \end{cases} \tag{2}$$

where r is the radius of the earth. Taking the square for both sides of (1) and substituting the relevant terms with (2), we have the initial location equations

$${\rho_i}^2 - {r_i}^2 - r^2 = -2(x_i x_t + y_i y_t + z_i z_t). \tag{3}$$

The equations are expressed as follows:

$$\begin{cases} {\rho_1}^2 - {r_1}^2 - r^2 = -2(x_1 x_t + y_1 y_t + z_1 z_t), \\ {\rho_2}^2 - {r_2}^2 - r^2 = -2(x_2 x_t + y_2 y_t + z_2 z_t), \\ {\rho_3}^2 - {r_3}^2 - r^2 = -2(x_3 x_t + y_3 y_t + z_3 z_t). \end{cases} \tag{4}$$

Eq. (4) can also be expressed in vector form as

$$\boldsymbol{A}_1 \boldsymbol{x}_t = \boldsymbol{B}_1, \tag{5}$$

where

$$\boldsymbol{B}_1 = \begin{bmatrix} {\rho_1}^2 - {r_1}^2 - r^2 \\ {\rho_2}^2 - {r_2}^2 - r^2 \\ {\rho_3}^2 - {r_3}^2 - r^2 \end{bmatrix}, \quad \boldsymbol{A}_1 = \begin{bmatrix} -2x_1 & -2y_1 & -2z_1 \\ -2x_2 & -2y_2 & -2z_2 \\ -2x_3 & -2y_3 & -2z_3 \end{bmatrix}, \quad \boldsymbol{x}_t = \begin{bmatrix} x_t \\ y_t \\ z_t \end{bmatrix}.$$

To obtain $\boldsymbol{x}_t$, both sides of (5) are multiplied by ${\boldsymbol{A}_1}^{-1}$, giving

$$\boldsymbol{x}_t = {\boldsymbol{A}_1}^{-1} \cdot \boldsymbol{B}_1. \tag{6}$$

Now, an approximate estimation of the target location can be calculated. Let $\boldsymbol{x}_0 = \boldsymbol{x}_t$, and in the following algorithm, apply the results in a Taylor series.

2.2.2 *Expression of the location solution*

The relative distance ρ_i between the target and UAV$_i$ can be expressed as

$$\rho_i = \|\boldsymbol{x}_i - \boldsymbol{x}_t\| + \varepsilon_{\rho i}, \quad i = 1, 2, 3. \tag{7}$$

Assume that $\varepsilon_{\rho i}$ is the measurement error of UAV$_i$, which has a Gaussian random distribution with zero mean and variance σ_ρ^2. Let us expand the right-hand side of (7) in a Taylor series for $\boldsymbol{x}_0 = [x_0, y_0, z_0]^{\mathrm{T}}$, and neglect higher order terms.

$$\rho_i = \|\boldsymbol{x}_i - \boldsymbol{x}_0\| - \frac{(x_i - x_0)(x_t - x_0)}{\|\boldsymbol{x}_i - \boldsymbol{x}_0\|} - \frac{(y_i - y_0)(y_t - y_0)}{\|\boldsymbol{x}_i - \boldsymbol{x}_0\|} - \frac{(z_i - z_0)(z_t - z_0)}{\|\boldsymbol{x}_i - \boldsymbol{x}_0\|} + \varepsilon_{\rho i}. \tag{8}$$

Define

$$\|\boldsymbol{x}_i - \boldsymbol{x}_0\| = \rho_i *. \tag{9}$$

From (8) and (9), a location equation in vector format can be obtained as

$$\boldsymbol{A}\boldsymbol{y} = \boldsymbol{B}, \tag{10}$$

where

$$\boldsymbol{A}=\begin{bmatrix} \frac{x_1-x_0}{\rho_1^*} & \frac{y_1-y_0}{\rho_1^*} & \frac{z_1-z_0}{\rho_1^*} \\ \frac{x_2-x_0}{\rho_2^*} & \frac{y_2-y_0}{\rho_2^*} & \frac{z_2-z_0}{\rho_2^*} \\ \frac{x_3-x_0}{\rho_3^*} & \frac{y_3-y_0}{\rho_3^*} & \frac{z_3-z_0}{\rho_3^*} \end{bmatrix}, \quad \boldsymbol{y}=\begin{bmatrix} x_t-x_0 \\ y_t-y_0 \\ z_t-z_0 \end{bmatrix}, \quad \boldsymbol{B}=\begin{bmatrix} \rho_1^*-\rho_1+\varepsilon_{\rho 1} \\ \rho_2^*-\rho_2+\varepsilon_{\rho 2} \\ \rho_3^*-\rho_3+\varepsilon_{\rho 3} \end{bmatrix}.$$

To reckon $\tilde{\boldsymbol{y}}$, similar to (6), we have

$$\tilde{\boldsymbol{y}}=\boldsymbol{A}^{-1}\boldsymbol{B}. \tag{11}$$

Now, the solution to the location equation is calculated, the data preparation for which applies the following algorithm.

Then, a complete location equation is obtained by introducing the UAV position errors into the location equation (10). Assuming that the UAV position errors $\Delta\boldsymbol{x}_i$ have an uncorrelated Gaussian random distribution with zero mean and variance σ_i^2, it is thus clear that a noise disturbance occurs in vectors $\boldsymbol{A}$ and $\boldsymbol{B}$ of (11). Let $\Delta\boldsymbol{x}_i=[\,\Delta x_i\ \Delta y_i\ \Delta z_i\,]^{\mathrm{T}}$, leading into (10), and then the equation is expressed as

$$\begin{bmatrix} \frac{x_i-x_0}{\rho_i*}-\boldsymbol{a}_i\cdot\Delta\boldsymbol{x}_i & \frac{y_i-y_0}{\rho_i*}-\boldsymbol{b}_i\cdot\Delta\boldsymbol{x}_i & \frac{z_i-z_0}{\rho_i*}-\boldsymbol{c}_i\cdot\Delta\boldsymbol{x}_i \end{bmatrix}\begin{bmatrix} x_t-x_0 \\ y_t-y_0 \\ z_t-z_0 \end{bmatrix}=\rho_i*-\boldsymbol{d}_i\Delta\boldsymbol{x}_i-\rho_i+\varepsilon_{\rho i}, \tag{12}$$

where

$$\boldsymbol{a}_i=\frac{\partial(\frac{x_i-x_0}{\rho_i*})}{\partial\Delta\boldsymbol{x}_i}=\begin{bmatrix} \frac{1}{\rho_i*}-\frac{(x_i-x_0)^2}{(\rho_i*)^3} & -\frac{(x_i-x_0)(y_i-y_0)}{(\rho_i*)^3} & -\frac{(x_i-x_0)(z_i-z_0)}{(\rho_i*)^3} \end{bmatrix}, \tag{13}$$

$$\boldsymbol{b}_i=\frac{\partial(\frac{y_i-y_0}{\rho_i*})}{\partial\Delta\boldsymbol{x}_i}=\begin{bmatrix} -\frac{(x_i-x_0)(y_i-y_0)}{(\rho_i*)^3} & \frac{1}{\rho_i*}-\frac{(y_i-y_0)^2}{(\rho_i*)^3} & -\frac{(y_i-y_0)(z_i-z_0)}{(\rho_i*)^3} \end{bmatrix}, \tag{14}$$

$$\boldsymbol{c}_i=\frac{\partial(\frac{z_i-z_0}{\rho_i*})}{\partial\Delta\boldsymbol{x}_i}=\begin{bmatrix} -\frac{(x_i-x_0)(z_i-z_0)}{(\rho_i*)^3} & -\frac{(y_i-y_0)(z_i-z_0)}{(\rho_i*)^3} & \frac{1}{\rho_i*}-\frac{(z_i-z_0)^2}{(\rho_i*)^3} \end{bmatrix}, \tag{15}$$

$$\boldsymbol{d}_i=\frac{\partial\rho_i*}{\partial\Delta\boldsymbol{x}_i}=\begin{bmatrix} \frac{x_i-x_0}{\rho_i*} & \frac{y_i-y_0}{\rho_i*} & \frac{z_i-z_0}{\rho_i*} \end{bmatrix}. \tag{16}$$

From the equations above, an error equation in symbolic form is

$$(\boldsymbol{A}-\Delta\boldsymbol{A})\,\boldsymbol{y}=(\boldsymbol{B}-\Delta\boldsymbol{B})\,. \tag{17}$$

Let

$$\begin{cases} \Delta\boldsymbol{x}=[\,\Delta\boldsymbol{x}_1\ \Delta\boldsymbol{x}_2\ \Delta\boldsymbol{x}_3\,]^{\mathrm{T}}, \\ \boldsymbol{G}_1=\mathrm{diag}[\,\boldsymbol{a}_1\ \boldsymbol{a}_2\ \boldsymbol{a}_3\,], \\ \boldsymbol{G}_2=\mathrm{diag}[\,\boldsymbol{b}_1\ \boldsymbol{b}_2\ \boldsymbol{b}_3\,], \\ \boldsymbol{G}_3=\mathrm{diag}[\,\boldsymbol{c}_1\ \boldsymbol{c}_2\ \boldsymbol{c}_3\,], \\ \boldsymbol{G}_4=\mathrm{diag}[\,\boldsymbol{d}_1\ \boldsymbol{d}_2\ \boldsymbol{d}_3\,], \\ \boldsymbol{A}^*=\boldsymbol{A}-\Delta\boldsymbol{A}, \\ \boldsymbol{B}^*=\boldsymbol{B}-\Delta\boldsymbol{B}. \end{cases} \tag{18}$$

Then, $\Delta\boldsymbol{A}$ and $\Delta\boldsymbol{B}$ of (17) can be expressed as

$$\begin{cases} \Delta\boldsymbol{A}=[\,\boldsymbol{a}_i\cdot\Delta\boldsymbol{x}_i\ \boldsymbol{b}_i\cdot\Delta\boldsymbol{x}_i\ \boldsymbol{c}_i\cdot\Delta\boldsymbol{x}_i\,]=[\,\boldsymbol{G}_1\cdot\Delta\boldsymbol{x}\ \boldsymbol{G}_2\cdot\Delta\boldsymbol{x}\ \boldsymbol{G}_3\cdot\Delta\boldsymbol{x}\,], \\ \Delta\boldsymbol{B}=[\boldsymbol{d}_i\cdot\Delta\boldsymbol{x}_i]=[\boldsymbol{G}_4\cdot\Delta\boldsymbol{x}]\,. \end{cases} \tag{19}$$

Eqs. (18)–(20) can infer the following:

$$\boldsymbol{A}^*\boldsymbol{y}=\boldsymbol{B}^*. \tag{20}$$

To reckon $\boldsymbol{y}$, let $\boldsymbol{H}_y = x\boldsymbol{G}_1 + y\boldsymbol{G}_2 + z\boldsymbol{G}_3 - \boldsymbol{G}_4$, where (x, y, z) indicates the data preparation in (11), and the solution to the proposed algorithm is therefore

$$\begin{cases} \min(\|\Delta\boldsymbol{x}\|_2^2 + \lambda\|\boldsymbol{y}\|_2^2), \\ \text{s.t. } \boldsymbol{A}\boldsymbol{y} - \boldsymbol{B} + \boldsymbol{H}_y\Delta\boldsymbol{x} = \boldsymbol{0}. \end{cases} \tag{21}$$

It is clear that $\boldsymbol{H}_y$ must be a diagonal matrix, and that its diagonal elements are not 0, and thus ${\boldsymbol{H}_y}^{-1}$ can be calculated. Then, Eq. (22) will lead to

$$\begin{cases} \Delta\boldsymbol{x} = -\boldsymbol{H}_y^{-1}(\boldsymbol{A}\boldsymbol{y} - \boldsymbol{B}), \\ \|\Delta\boldsymbol{x}\|_2^2 = \Delta\boldsymbol{x}^{\mathrm{T}} \cdot \Delta\boldsymbol{x} = (\boldsymbol{A}\boldsymbol{y} - \boldsymbol{B})^{\mathrm{T}}\boldsymbol{H}_y^{-2}(\boldsymbol{A}\boldsymbol{y} - \boldsymbol{B}). \end{cases} \tag{22}$$

By substituting the relevant terms in (21) with (22), the solution vector of (21) can be expressed as

$$\boldsymbol{y}_{\mathrm{TLS}} = \arg\min\left(\|\Delta\boldsymbol{x}\|_2^2 + \lambda\|\boldsymbol{y}\|_2^2\right) = \arg\min\left[(\boldsymbol{A}\boldsymbol{y} - \boldsymbol{B})^{\mathrm{T}}\boldsymbol{H}_y^{-2}(\boldsymbol{A}\boldsymbol{y} - \boldsymbol{B}) + \lambda\boldsymbol{y}^{\mathrm{T}}\boldsymbol{y}\right]. \tag{23}$$

To calculate $\boldsymbol{y}_{\mathrm{TLS}}$, a derivation is taken as

$$\frac{\partial\left(\|\Delta\boldsymbol{x}\|_2^2 + \lambda\|\boldsymbol{y}\|_2^2\right)}{\partial\boldsymbol{y}} = \left[2\boldsymbol{A}^{\mathrm{T}}\boldsymbol{H}_y^{-2}(\boldsymbol{A}\boldsymbol{y} - \boldsymbol{B}) + (\boldsymbol{A}\boldsymbol{y} - \boldsymbol{B})^{\mathrm{T}}\frac{\partial\boldsymbol{H}_y^{-2}}{\partial\boldsymbol{y}}(\boldsymbol{A}\boldsymbol{y} - \boldsymbol{B}) + 2\lambda\boldsymbol{y}\right] = 0, \tag{24}$$

for which

$$\begin{aligned} &(\boldsymbol{A}\boldsymbol{y} - \boldsymbol{B})^{\mathrm{T}}\frac{\partial\boldsymbol{H}_y^{-2}}{\partial\boldsymbol{y}}(\boldsymbol{A}\boldsymbol{y} - \boldsymbol{B}) \\ &= (\boldsymbol{A}\boldsymbol{y} - \boldsymbol{B})^{\mathrm{T}}\frac{\partial\boldsymbol{H}_y^{-2}}{\partial(x - x_0)}(\boldsymbol{A}\boldsymbol{y} - \boldsymbol{B}) + (\boldsymbol{A}\boldsymbol{y} - \boldsymbol{B})^{\mathrm{T}}\frac{\partial\boldsymbol{H}_y^{-2}}{\partial(y - y_0)}(\boldsymbol{A}\boldsymbol{y} - \boldsymbol{B}) + (\boldsymbol{A}\boldsymbol{y} - \boldsymbol{B})^{\mathrm{T}}\frac{\partial\boldsymbol{H}_y^{-2}}{\partial(z - z_0)}(\boldsymbol{A}\boldsymbol{y} - \boldsymbol{B}). \end{aligned} \tag{25}$$

Neglecting the cross terms and small quantities of (25), Eq. (24) becomes

$$\boldsymbol{A}^{\mathrm{T}}\boldsymbol{H}_y^{-2}\boldsymbol{A}\boldsymbol{y} + \lambda\boldsymbol{y} = \boldsymbol{A}^{\mathrm{T}}\boldsymbol{H}_y^{-2}\boldsymbol{B}. \tag{26}$$

The expression of the location solution can be inferred as follows:

$$\boldsymbol{y}_{\mathrm{TLS}} = \left(\boldsymbol{A}^{\mathrm{T}}\boldsymbol{H}_y^{-2}\boldsymbol{A} + \lambda I\right)^{-1}\boldsymbol{A}^{\mathrm{T}}\boldsymbol{H}_y^{-2}\boldsymbol{B}, \tag{27}$$

where $\boldsymbol{A}, \boldsymbol{B}$, and $\boldsymbol{H}_y$ are known from the relative distance, position of the UAVs, and data preparation in (11). However, the value of λ is still unknown.

2.2.3 *Solving the value of* λ

Let

$$\boldsymbol{y}_{\mathrm{TLS}} = \boldsymbol{y}^* + \delta\boldsymbol{y}, \tag{28}$$

where $\boldsymbol{y}^*$ is the true value of $\boldsymbol{y}$, and $\delta\boldsymbol{y}$ is the deviation of $\boldsymbol{y}_{\mathrm{TLS}}$ and $\boldsymbol{y}^*$; thus, substituting (26) into (24) gives

$$\boldsymbol{A}^{\mathrm{T}}\boldsymbol{H}_y^{-2}\left(\boldsymbol{A}\boldsymbol{y}^* + \boldsymbol{A}\delta\boldsymbol{y} - \boldsymbol{B}\right) + \lambda\left(\boldsymbol{y}^* + \delta\boldsymbol{y}\right) = 0. \tag{29}$$

From (18), (20) and (29), Eqs. (30) and (31) can be obtained as

$$\boldsymbol{A}^{\mathrm{T}}\boldsymbol{H}_y^{-2}\left(\Delta\boldsymbol{A}\boldsymbol{y}^* + \boldsymbol{A}^*\delta\boldsymbol{y} - \Delta\boldsymbol{B}\right) + \lambda\left(\boldsymbol{y}^* + \delta\boldsymbol{y}\right) = 0, \tag{30}$$

$$-\boldsymbol{H}_y\Delta\boldsymbol{x} = \left(\boldsymbol{A}^* + \Delta\boldsymbol{A}\right)\boldsymbol{y} - \left(\boldsymbol{B}^* + \Delta\boldsymbol{B}\right) = \left(\boldsymbol{A}^*\boldsymbol{y} - \boldsymbol{B}^*\right) + \Delta\boldsymbol{A}\boldsymbol{y} - \Delta\boldsymbol{B} = \Delta\boldsymbol{A}\boldsymbol{y}^* - \Delta\boldsymbol{B}\,. \tag{31}$$

Substituting (31) into (30) will be expressed as

$$\boldsymbol{A}^{*\mathrm{T}}A_y^{-2}\left(\boldsymbol{A}^*\delta\boldsymbol{y} - \boldsymbol{H}_y\Delta\boldsymbol{x}\right) + \lambda\left(\boldsymbol{y}^* + \delta\boldsymbol{y}\right) = 0. \tag{32}$$

Eq. (32) can be deformed as

$$\delta \boldsymbol{y} = \left(\boldsymbol{A}^{*\mathrm{T}} \boldsymbol{H}_y^{-2} \boldsymbol{A}^* + \lambda I\right)^{-1} \left(\boldsymbol{A}^{*\mathrm{T}} \boldsymbol{H}_y^{-1} \Delta \boldsymbol{x} - \lambda \boldsymbol{y}^*\right). \tag{33}$$

The mean square error $\delta \boldsymbol{y}$ is as follows:

$$\begin{aligned} &\mathrm{MSE}\left(\delta \boldsymbol{y}\right) = \mathrm{E}\left(\delta \boldsymbol{y}^{\mathrm{T}} \delta \boldsymbol{y}\right) \\ &= \mathrm{E}\left[\left(\boldsymbol{A}^{*\mathrm{T}} \boldsymbol{H}_y^{-1} \Delta \boldsymbol{x} - \lambda \boldsymbol{y}^*\right)^{\mathrm{T}} \left(\left(\boldsymbol{A}^{*\mathrm{T}} \boldsymbol{H}_y^{-2} \boldsymbol{A}^* + \lambda I\right)^{-1}\right)^{\mathrm{T}} \left(\boldsymbol{A}^{*\mathrm{T}} \boldsymbol{H}_y^{-2} \boldsymbol{A}^* + \lambda I\right)^{-1} \left(\boldsymbol{A}^{*\mathrm{T}} \boldsymbol{H}_y^{-1} \Delta \boldsymbol{x} - \lambda \boldsymbol{y}^*\right)\right]. \end{aligned} \tag{34}$$

It is obvious that this is a symmetric matrix, and the following equation can be obtained

$$\left(\boldsymbol{A}^{*\mathrm{T}} \boldsymbol{H}_y^{-2} \boldsymbol{A}^* + \lambda I\right)^{-1} = \left(\left(\boldsymbol{A}^{*\mathrm{T}} \boldsymbol{H}_y^{-2} \boldsymbol{A}^* + \lambda I\right)^{-1}\right)^{\mathrm{T}}. \tag{35}$$

Substituting (35) into (34) gives a reduction of (34):

$$\begin{aligned} \mathrm{MSE}\left(\delta \boldsymbol{y}\right) =& \lambda^2 \boldsymbol{y}^{*\mathrm{T}} \left(\boldsymbol{A}^{*\mathrm{T}} \boldsymbol{H}_y^{-2} \boldsymbol{A}^* + \lambda I\right)^{-2} \boldsymbol{y}^* \\ &+ \mathrm{E}\left[\Delta \boldsymbol{x}^{\mathrm{T}} \boldsymbol{H}_y^{-1} \boldsymbol{A}^* \left(\boldsymbol{A}^{*\mathrm{T}} \boldsymbol{H}_y^{-2} \boldsymbol{A}^* + \lambda I\right)^{-2} \boldsymbol{A}^{*\mathrm{T}} \boldsymbol{H}_y^{-1} \Delta \boldsymbol{x}\right]. \end{aligned} \tag{36}$$

Because it is virtually impossible to obtain the real values ($\boldsymbol{A}^*$), the measured values ($\boldsymbol{A}$) can be used instead. Moreover, the value of λ can be calculated as follows:

$$\begin{aligned} \hat{\lambda} &= \arg\min_{\lambda} \left[\mathrm{MSE}(\delta \boldsymbol{y})\right] \\ &= \arg\min_{\lambda} \{[\lambda^2 \boldsymbol{y}^{\mathrm{T}} (\boldsymbol{A}^{\mathrm{T}} \boldsymbol{H}_y^{-2} \boldsymbol{A} + \lambda I)^{-2} \boldsymbol{y}] + \mathrm{E}[\Delta \boldsymbol{x}^{\mathrm{T}} \boldsymbol{H}_y^{-1} \boldsymbol{A} (\boldsymbol{A}^{\mathrm{T}} \boldsymbol{H}_y^{-2} \boldsymbol{A} + \lambda I)^{-2} \boldsymbol{A}^{\mathrm{T}} \boldsymbol{H}_y^{-1} \Delta \boldsymbol{x}]\}. \end{aligned} \tag{37}$$

Define

$$\begin{cases} p = \lambda^2 \boldsymbol{y}^{\mathrm{T}} \left(\boldsymbol{A}^{\mathrm{T}} \boldsymbol{H}_y^{-2} \boldsymbol{A} + \lambda I\right)^{-2} \boldsymbol{y}, \\ q = \mathrm{E}[\Delta \boldsymbol{x}^{\mathrm{T}} \boldsymbol{H}_y^{-1} \boldsymbol{A} (\boldsymbol{A}^{\mathrm{T}} \boldsymbol{H}_y^{-2} \boldsymbol{A} + \lambda I)^{-2} \boldsymbol{A}^{\mathrm{T}} \boldsymbol{H}_y^{-1} \Delta \boldsymbol{x}]. \end{cases} \tag{38}$$

Obtaining the diagonalization of $\boldsymbol{A}^{\mathrm{T}} \boldsymbol{H}_y^{-2} \boldsymbol{A}$ gives

$$\boldsymbol{A}^{\mathrm{T}} \boldsymbol{H}_y^{-2} \boldsymbol{A} = Q^{\mathrm{T}} \Lambda Q = Q^{\mathrm{T}} \mathrm{diag}\left(\mu_1, \mu_2, \mu_3\right) Q, \tag{39}$$

and $(\boldsymbol{A}^{\mathrm{T}} \boldsymbol{H}_y^{-2} \boldsymbol{A} + \lambda I)^{-2}$ can be expressed as

$$(\boldsymbol{A}^{\mathrm{T}} \boldsymbol{H}_y^{-2} \boldsymbol{A} + \lambda I)^{-2} = Q^{\mathrm{T}} \mathrm{diag}\left[(\mu_1 + \lambda)^{-2}, (\mu_2 + \lambda)^{-2}, (\mu_3 + \lambda)^{-2}\right] Q = Q^{\mathrm{T}} D Q\,, \tag{40}$$

where

$$D = \mathrm{diag}\left[(\mu_1 + \lambda)^{-2}, (\mu_2 + \lambda)^{-2}, (\mu_3 + \lambda)^{-2}\right]. \tag{41}$$

Finally, substituting (40) into (38) gives

$$\begin{cases} p = \lambda^2 \boldsymbol{y}^{\mathrm{T}} Q^{\mathrm{T}} D Q \boldsymbol{y} = \lambda^2 (Q \boldsymbol{y})^{\mathrm{T}} D Q \boldsymbol{y}, \\ q = \mathrm{E}[\Delta \boldsymbol{x}^{\mathrm{T}} \boldsymbol{H}_y^{-1} \boldsymbol{A} Q^{\mathrm{T}} D Q \boldsymbol{A}^{\mathrm{T}} \boldsymbol{H}_y^{-1} \Delta \boldsymbol{x}] = \mathrm{E}[(Q \boldsymbol{A}^{\mathrm{T}} \boldsymbol{H}_y^{-1} \Delta \boldsymbol{x})^{\mathrm{T}} D Q \boldsymbol{A}^{\mathrm{T}} \boldsymbol{H}_y^{-1} \Delta \boldsymbol{x}]. \end{cases} \tag{42}$$

Let C_1 and C_2 be two column vectors that satisfy the following expressions, $C_1 = Q \boldsymbol{y}$ and $C_2 = Q \boldsymbol{A}^{\mathrm{T}} \boldsymbol{H}_y^{-1} \Delta \boldsymbol{x}$, where

$$\begin{cases} C_1 = \begin{pmatrix} c_{11} & c_{12} & c_{13} \end{pmatrix}^{\mathrm{T}}, \\ C_2 = \begin{pmatrix} c_{21} & c_{22} & c_{23} \end{pmatrix}^{\mathrm{T}}. \end{cases} \tag{43}$$

According to [14], the MSE($\delta \boldsymbol{y}$) has a unique minimum in this interval, namely,

$$\left[\min \frac{\mathrm{E}\left\{c_{1i}^2\right\}}{c_{2i}^2 \mu_i}, \max \frac{\mathrm{E}\left\{c_{1i}^2\right\}}{c_{2i}^2 \mu_i}\right], \quad i = 1, 2, 3. \tag{44}$$

In addition, in the present paper, the value of λ is chosen as

$$\hat{\lambda} = \frac{1}{2}\min\frac{\mathrm{E}\left\{c_{1i}^2\right\}}{c_{2i}^2\mu_i} + \frac{1}{2}\max\frac{\mathrm{E}\left\{c_{1i}^2\right\}}{c_{2i}^2\mu_i}. \tag{45}$$

Substituting the value of λ into (27), the location solution of the target can be calculated.

As a summary, the solution of the location is listed as

$$\boldsymbol{y}_{\mathrm{TLS}} = \left(\boldsymbol{A}^{\mathrm{T}}\boldsymbol{H}_y^{-2}\boldsymbol{A} + \left(\frac{1}{2}\min\frac{\mathrm{E}\left\{c_{1i}^2\right\}}{c_{2i}^2\mu_i} + \frac{1}{2}\max\frac{\mathrm{E}\left\{c_{1i}^2\right\}}{c_{2i}^2\mu_i}\right)I\right)^{-1}\boldsymbol{A}^{\mathrm{T}}\boldsymbol{H}_y^{-2}\boldsymbol{B}. \tag{46}$$

Thus far, the solution of the target has been calculated through the proposed method; its performance will be analyzed in the following sections.

3 Simulation and analysis

From the location algorithm above, the cooperative location accuracy is impacted through three factors, namely, the UAV position errors, measurement errors, and the flight altitude. The influences of these factors are thus analyzed successively, and feasible regions of these factors can be determined for the location accuracy requirement.

3.1 Assumption

To validate the proposed method through a simulation, the following assumptions are made.

Assumption 1. Three UAVs fly around the target and maintain the formation of the UAVs.

Assumption 2. The position measurement and measurement errors of each UAV have the same measurement covariance:

$$\begin{cases} {\sigma_i}^2 = \sigma_1^2, \\ {\sigma_\rho}^2 = \sigma_2^2, \end{cases} \quad (i = 1, 2, 3).$$

Assumption 3. The coordinate system is defined as the geocentric coordinate system, namely, the coordinate origin at the center of the earth, and we assume that the earth is a homogeneous sphere whose radius is the average radius:

$$r = 6371.004 \text{ km}.$$

Assumption 4. The setting requirement of the location accuracy is less than 10 m.

3.2 Simulation results

3.2.1 *Analysis of effectiveness and suitability of the proposed method*

The proposed method described herein is implemented using the location algorithm above, and the Grewal MS method, which was introduced in Subsection 2.2. Then, assume that the real location of the target is $\boldsymbol{x} = (6371, 20, 0.02)$ and that the initial locations of three UAVs are as listed in Table 1. Comparisons of the location accuracy between the proposed and Grewal MS methods are conducted based on two aspects: the UAV position errors can be ignored, the result of which is shown in Figure 2, or the UAV position errors are too large to ignore, the result of which is shown in Figure 3.

Figure 2 shows the simulation results when the measurement errors are uniformly distributed on $[0, 0.01]$ during each trial. Again, the proposed technique is more accurate at medium to high measurement errors, and close to the Grewal MS method at low to medium measurement errors. Thus it is obvious that the proposed method behaves better when the UAV position errors are zero. It can be clearly seen that the location accuracy of the Grewal MS method is limited by the precision of the earth's radius, which introduces errors in the processing of the algorithm. In addition, the accuracy of the proposed method is insensitive to the positioning results of the Grewal MS method; in other words, the accuracy of the

Table 1 Initial locations of UAVs

UAV	Location (km, km, km)
UAV1	(6370.1, 19.5, 1)
UAV2	(6371.9, 19.5, 1)
UAV3	(6371.1, 20.9, 1)

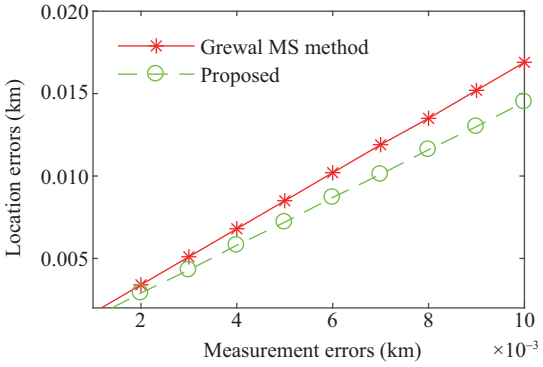

Figure 2 (Color online) Location accuracy of the proposed method compared to the Grewal MS method when the UAV position errors are ignored.

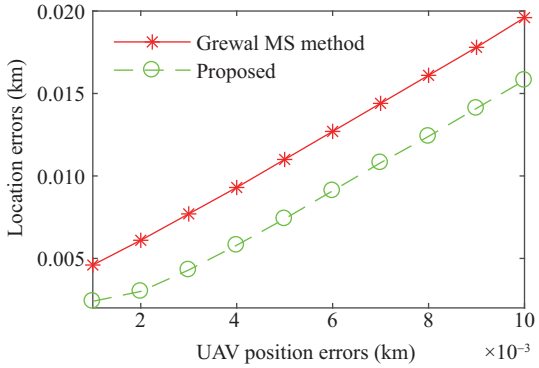

Figure 3 (Color online) Location accuracy of the proposed method compared to the Grewal MS method when the UAV position errors cannot be ignored.

earth's radius has little effect on the precision of its solution. Therefore, the proposed method is more effective than the Grewal MS method.

Then, the UAV position errors are added to the simulation and measurement errors, which are fixed as $\sigma_2 = 0.002$. As shown in Figure 3, the difference in location accuracy is significantly increased when compared with Figure 2, indicating that the Grewal MS method is more sensitive to the increase in the UAV position errors than the proposed method. Evidently, the proposed method is much more accurate at low to medium UAV position errors.

3.2.2 *Influence of measurement errors and UAV position errors on the accuracy*

The main idea here is to analyze such influence as follows:

(a) Set the initial values of the three factors.

(b) Let the covariance of the measurement errors satisfy the following equation, $0.001 \leqslant \sigma_2 \leqslant 0.01$, and finish the simulation.

(c) Add 0.001 to σ_1 and repeat (b) until $\sigma_1 = 0.008$.

(d) The initial feasible region of the measurement errors is obtained by combining all of the simulation results above.

All of the simulation results are shown in Figure 4.

As Figure 4 shows, every curve maps a value of σ_1 from 0.001 to 0.008, and with an increase in σ_2 from 0.001 to 0.01, the location error also increases in the overall trend. Through an analysis of $\sigma_1 = 0.006$, we can see that the location errors slightly decrease initially, and then increase as σ_2 increases, and the value of the location errors will be less than 0.010 km if $\sigma_2 < 0.006$.

3.2.3 *Influence of flight altitude on accuracy*

Assuming h is uniformly distributed on $[1, 10]$ and other two factors satisfy $\sigma_1 = \sigma_2 = 0.002$, the influence of h on the accuracy can then be expressed.

Figure 5 shows simulation results when h is uniformly distributed on $[1, 10]$ during each trial. Again, the location errors decrease with the increase in h. More concretely, the higher the UAVs fly, the smaller the location errors that occur.

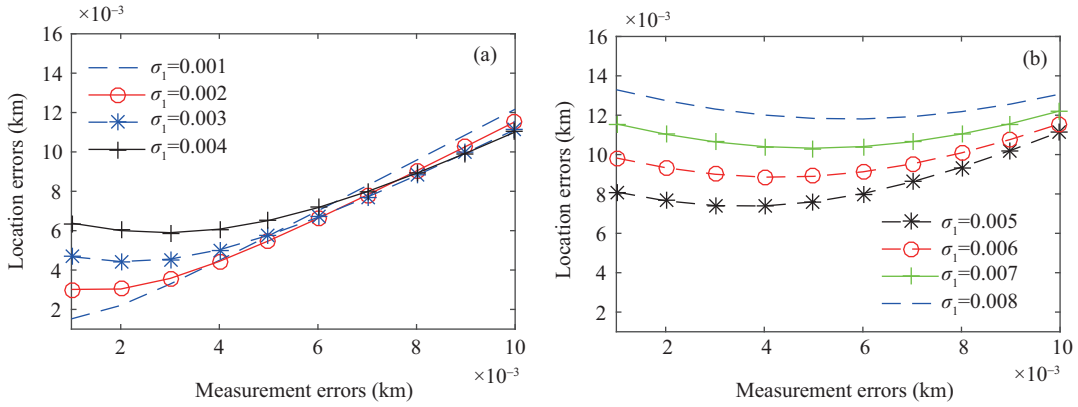

Figure 4 (Color online) Location errors mapped with measurement errors. (a) $\sigma_1 = 0.001, 0.002, 0.003, 0.004$; (b) $\sigma_1 = 0.005, 0.006, 0.007, 0.008$.

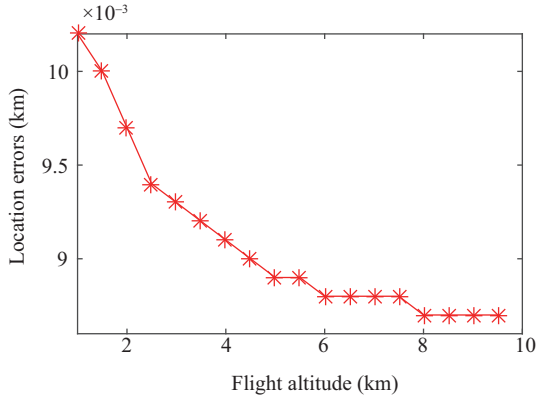

Figure 5 (Color online) Location errors based on the flight altitude.

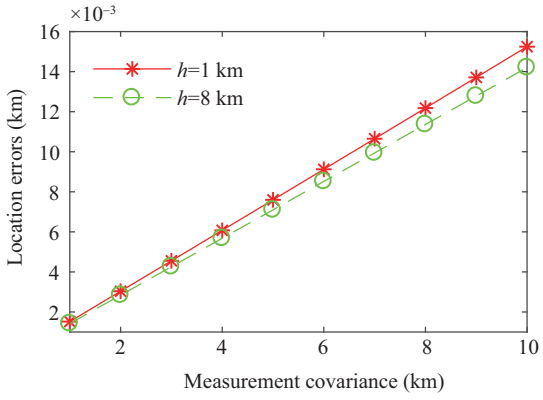

Figure 6 (Color online) Comparison of accuracy between flight altitude of 1 km and flight altitude of 8 km when σ is random.

An overall consideration of the influence should be given by adding the UAV position errors and the measurement errors. Assume that they satisfy $\sigma_1 = \sigma_2 = \sigma$, where σ^2 indicates the measurement covariance.

From Figure 6, the location errors decrease with the increase in the measurement covariance. Moreover, the location errors of $h = 8$ km are more accurate at medium to high measurement covariance, and are close to the location errors of $h = 1$ km at low to medium measurement covariance, which also indicates that the higher the UAVs fly, the smaller the location errors that occur.

3.3 Results analysis

From Figures 2 and 3, the excellent performance of the proposed method is proved, and regardless of whether the influence of the UAV position errors is considered, the proposed method is much more accurate than the Grewal MS method.

As shown in Figure 4, the smaller σ_2 is, the smaller the location errors that occur. Moreover, combining all the simulation results, the location accuracy can satisfy the location accuracy requirement if $\sigma_1 \leqslant 0.006$ km and $\sigma_2 \leqslant 0.006$ km. As a supplement, the simulations are based on $h = 1$ km, which means the conclusion is only an initial feasible region.

Figure 5 shows that the location errors decrease with the increase in h. More concretely, the errors decrease sharply at low to medium elevation but decrease slightly at medium to high elevation. In other words, the location accuracy of $h \geqslant 1$ km can absolutely satisfy the location accuracy requirement when

$h = 1$ km. Thus, the feasible regions can be concluded as follows: $\sigma_1 \leqslant 0.006$ km, $\sigma_2 \leqslant 0.006$ km, and $h \geqslant 1$ km. Furthermore, Figure 6 verifies the conclusion that the location accuracy will satisfy the requirement if all factors are within the feasible region.

4 Conclusion

We proposed a ground target cooperative localization method, the effectiveness and benefits of which were proved through a comparison with a traditional method. As a demonstration illustrating how to deduce the feasible regions, the value regions of the key factors were determined for the location accuracy requirement. Once all factors are within the feasible regions, the location accuracy will certainly satisfy the requirement.

Acknowledgements This work was supported by National Natural Science Foundation of China (Grant No. 61473229).

References

1 Li P, Yu X, Peng X Y, et al. Fault-tolerant cooperative control for multiple UAVs based on sliding mode techniques. Sci China Inf Sci, 2017, 60: 070204
2 Zhang Y Z, Hu B, Li J W, et al. UAV multi-mission reconnaissance decision-making under uncertainty environment. J Northwestern Polytechnical Univ, 2016, 34: 1028–1034
3 He W, Huang H, Chen Y, et al. Development of an autonomous flapping-wing aerial vehicle. Sci China Inf Sci, 2017, 60: 063201
4 Li C Q, Li X B, Zhang J, et al. Analysis of airborne passive location precision based on multi-static cooperation. Modern Radar, 2017, 39: 11–14
5 Zhu H M, Wang H Y, Sun S Y. Research on error correction method of single UAV based on Monte Carlo. Sci Tech Eng, 2017, 17: 255–259
6 Esmailifar S M, Saghafi F. Cooperative localization of marine targets by UAVs. Mech Syst Signal Process, 2017, 87: 23–42
7 Lee W, Bang H, Leeghim H. Cooperative localization between small UAVs using a combination of heterogeneous sensors. Aerospace Sci Tech, 2013, 27: 105–111
8 Wang K, Ke Y, Chen B M. Autonomous reconfigurable hybrid tail-sitter UAV U-Lion. Sci China Inf Sci, 2017, 60: 033201
9 Yang K, An J P, Bu X Y, et al. Constrained total least-squares location algorithm using time-difference-of-arrival measurements. IEEE Trans Veh Technol, 2010, 59: 1558–1562
10 Melchor-Aguilar D, Niculescu S I. Computing non-fragile PI controllers for delay models of TCP/AQM networks. Int J Control, 2009, 82: 2249–2259
11 Zhu G, Feng D, Yan Z, et al. TOA localization algorithm using the linear-correction technique. J Xidian Univ, 2015, 42: 22–25, 32
12 Grewal M S, Weill L R, Andrews A P. Global Positioning Systems, Inertial Navigation, and Integration. Hoboken: John Wiley & Sons, Inc., 2007, 3: 383–384
13 Li W C, Wei P, Xiao X C. A robust TDOA-based location method and its performance analysis. Sci China Ser F-Inf Sci, 2009, 52: 876–882
14 Fan X, Younan N H, Taylor C D. A perturbation analysis of the regularized constrained total least squares. IEEE Trans Circ Syst II, 1996, 43: 140–142